

SIMULATION OF AN RFQ FUNNEL FOR HEAVY-ION BEAMS*

F. W. Guy and R. H. Stokes

MS H817, Los Alamos National Laboratory, Los Alamos, NM 87545

Abstract

Use of the magnetic force to focus and deflect heavy-ion beams is marginal at low ion velocities. Low-emittance-growth funnels using discrete magnetic elements are difficult to design for these beams. We show that a new type of radio-frequency quadrupole (RFQ) funnel is especially suitable for this application. Simulation procedures, which include space-charge and image effects, have produced a high-quality funnel design for 20-MeV Bi^{+1} ions.

Introduction

In the radio-frequency (RF) linac approach to generating high-current ion beams for heavy-ion fusion, a main requirement is that many initial low-current beams be combined into a single, final beam. This scheme overcomes the beam-current limitations of both ion sources and low-velocity linear accelerators and will produce a single beam that can be efficiently accelerated to the final energy in a single-channel RF linac. To combine beams, a concept called "funneling" has been proposed. In this arrangement, pairs of bunched beams are combined by transverse deflections so that a single collinear beam with interlaced bunches is formed. The funneled beam is then suitable for further acceleration in a linac operating with twice the frequency of the two initial linacs that feed the funnel. After a suitable acceleration, this funneled beam can be combined with another funneled beam, and after multiple funnel stages, the final required beam current can be obtained. If beam loss and emittance growth are small during the funneling operation, each funneling stage results in an output beam with nearly twice the beam current and twice the transverse brightness. The funnel system must include adequate transverse and longitudinal focusing to prevent emittance growth during the funneling procedure.

A paper by Stovall, Guy, Stokes, and Wangler¹ discusses the funneling of Bi^{+1} ions. The authors found that for Bi^{+1} ions with an energy of 0.50 MeV/A, a funnel design could be developed using discrete-element funneling techniques (permanent magnet quadrupoles and dipoles and RF bunchers and deflectors.) Multiparticle beam simulations showed this funnel to have good performance; however, attempts to develop a low-emittance discrete-element funnel at lower energies were unsuccessful because of the limited magnetic focusing strength available for the lower velocity beams. This has suggested the application of RFQ funnel techniques that use electric forces to focus, deflect, and bunch the beam.

In the initial papers by Stokes and Minerbo^{2,3} discussing the RFQ funnel, the emphasis was placed on funneling two parallel, closely spaced beams that would be produced by a two-channel RFQ accelerator. This is shown schematically in the top half of Fig. 1. In the present study, we have chosen another, perhaps more realistic, arrangement where two separate RFQ accelerators produce slightly convergent beams that are combined by a different type of RFQ funnel. The funnel first provides deflection (and focusing) forces in separate RFQ channels that first make the two beams closely spaced and nearly parallel. Then the two beams enter a common channel where they are interlaced and made collinear. The arrangement is shown in the lower half of Fig. 1. This modified funnel is based on the alternative funneling potential function found in Ref. 3.

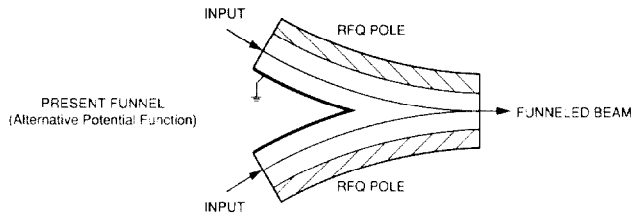
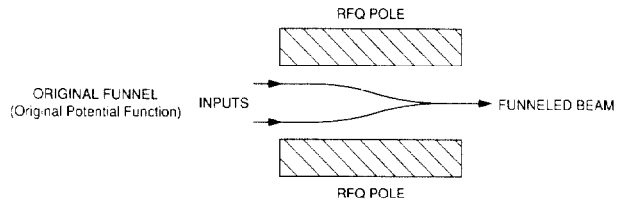


Fig. 1. RFQ funnels.

RFQ Funnel Techniques

The properties of an RFQ funnel that make it attractive for use as the first lowest velocity funnel stage have been described.^{2,3} These properties include the use of electric forces to focus and deflect the two beams and the ease of matching between the RFQ accelerator outputs and the funnel inputs. In addition, the RFQ funnel development is facilitated by the active widespread acceptance of the RFQ accelerator from which many design and engineering techniques can be borrowed.

In both the RFQ funnel and the RFQ accelerator, the beam dynamics and pole-tip designs are based upon appropriate potential functions. These potential functions satisfy Laplace's equation, and the beam dynamics designs and simulations use electric fields derived from the potential function expressions. In Appendix A of Ref. 3, an alternative funneling potential function is briefly discussed. The funnel design we present later is based upon this potential function, which can be written

$$U = \frac{V}{2} \left[G \frac{2xy}{a^2} + H \sinh kx \cos kz \right] \sin(\omega t + \phi), \quad (1)$$

where V is the maximum potential difference between adjacent poles, $k = 2\pi/\beta\lambda$, $\beta = v/c$, $\beta\lambda$ is the longitudinal space period (along the z -axis) of the modulated pole tips, and ω is the frequency of the pole-tip RF excitation. The electric field components calculated from Eq. (1) are

$$E_x = -\frac{GVy}{a^2} - \frac{HVk}{2} \cosh kx \cos kz, \quad E_y = -\frac{GVx}{a^2}, \quad (2)$$

and

$$E_z = \frac{HVk}{2} \sinh kx \sin kz$$

with each right-hand side multiplied by $\sin(\omega t + \phi)$. The second term in the expression for E_x is a dipole field that will be used to deflect the beams transversely in the x - z plane to produce a single funnel beam. The shape of the isopotential surfaces of the RFQ poles is obtained from Eq. (1) by setting $U(\text{max}) = V/2$, to obtain

$$\frac{G}{a^2} 2xy + H \sinh kx \cos kz = 1. \quad (3)$$

* Work supported by Los Alamos National Laboratory Program Development under the auspices of the US Department of Energy.

For $z = 0$, let $x = y = a/\sqrt{2}$; for $z = \beta\lambda/2$, let $x = y = ma/\sqrt{2}$, then

$$G = 1 - H \sinh \frac{ka}{\sqrt{2}}, \quad \text{and} \quad H = \frac{m^2 - 1}{m^2 \sinh \frac{ka}{\sqrt{2}} + \sinh \frac{mka}{\sqrt{2}}} \quad (4)$$

Because of the mirror symmetry of the potential function, if one pair of poles is replaced by a conducting y - z plane, the electric fields are preserved. Figure 2, which will be discussed later, includes plots in the x - y plane of one pair of RFQ funnel poles at three values of z . In these plots, the y -axis represents the position of the conducting plane. As the figure shows, the pole modulation is a sinusoidal-like displacement of both poles in the vertical direction with space period $\beta\lambda$. This displacement, together with the changing polarities of the two poles, produces an average dipole force in the x -direction. The amplitude of the pole displacement is a function of the modulation parameter m . If $m = 1$, ($G = 1$, $H = 0$), there is no dipole force. If $m > 1$, ($G < 1$, $H > 0$), then the poles are modulated and a dipole force is produced on a charged ion in the central region. Also, for appropriate values of the phase angle ϕ , the E_x field produces a bunching force that varies in strength with the x -displacement of the ions.

Numerical Calculation Procedure

The design problem was addressed numerically by a series of multiparticle simulations on three computer codes. A preliminary RFQ design was run on PARMTEQ, a code for generating and running RFQ problems; 4000 particles were started at the input of the RFQ. Transmitted particles were input into PARMILA, a linac and transport calculation code that transported them through a matching section comprising a drift, an electrostatic focusing quadrupole, and another drift. A randomly selected subset of 1000 particles was then fed into LIN, a code specialized for this RFQ funnel problem. PARMTEQ and PARMILA are standard Los Alamos design codes; the PARMILA version that we used has 3-D space charge. RFQ and matching section parameters are listed in Table I.

TABLE I. RFQ and Matching Section.

RFQ	Matching Section
Frequency: 10 MHz	Length: 16 cm
Current out: $I = 18.8$ mA	Aperture: 1.2 cm radius
Energy out: $W = 20$ MeV	Quadrupole voltage: 106
Aperture: $a = 1.3$ cm radius	Quadrupole length: 6 cm
Modulation parameter: $m = 1.6$	Transmission: 100%
Vane voltage: $V = 230$ kV	

LIN, the nonrelativistic code used for the funnel itself, transports a particle bunch through the structure of the funnel by discrete, small, time steps. At each time step, each particle's trajectory is acted upon by the electric fields of Eq. (2). These fields provide focusing, and the dipole portion of E_x causes particles to follow a curved path as indicated in Fig. 3. Particles are also affected by space charge and images. The 3-D space-charge effects are calculated by assuming each particle is a charge cloud of diameter approximately equal to the average Debye length in the bunch. Space-charge electric forces acting on a particle are summed from all the other particles in the bunch (interacting charge clouds). The charge cloud method minimizes collisional emittance growth by avoiding singularities for two close-together particles. Image charge effects are handled by a similar treatment whereby each particle sees images of every particle in the bunch as reflected in pole tips and the ground plane. Images strengthen longitudinal focusing and weaken transverse focusing; they also cause a shift in trajectory. Image effects are not large in this geometry but must be included because of the trajectory shift. For the image calculation, pole-tip shapes are approximated by cylinders tangent to the mathematically correct pole tips (the isopotential surfaces). Cylinder radius is $R = a\sqrt{m}$, and the point of tangency is $x = R/\sqrt{2}$. Outside a conducting cylinder, the image of a point charge generates a potential at a test point that is given by

$$U(\rho, r, z, \phi) = \frac{-q}{2\pi^2 \epsilon_0} \sum_{m=0}^{\infty} 2_m \cos(m\phi) \int_0^{\infty} \frac{I_m(kR)K_m(k\rho)K_m(kr)}{K_m(kR)} \cos(kz) dk, \quad (5)$$

where $2_0 = 1, 2_{m>0} = 2$,
 R is the cylinder radius,
 r is the radius of the test point,
 ρ is the radius of the charge,
 ϕ is the cylindrical coordinate angle between r and ρ ,
 z is the distance along the axis between charge and test point, and
 I and K are modified Bessel functions of the first and second kind.

Images in the ground plane are points at coordinates x, y, z of the image-generating charges. Electric fields from images in all appropriate surfaces are summed and applied at every time step. Also at every time step, beam envelopes and centroids are calculated and particles are tested for collision with pole tips and the ground plane.

Simulation Parameters

For this funnel design, the cell length was $\beta\lambda = 43$ cm. The beam line radius of curvature was set at $100\beta\lambda$ and the initial beam separation at 12.3 cm, reasonable for two rod-type low-frequency RFQs with RF feeds opposite each other. The aperture parameter "a" was taken as 1.455 cm to accommodate the beam from the matching section. The modulation parameter "m" was set at 1.325 and the intervane voltage V at 208 kV to obtain the correct

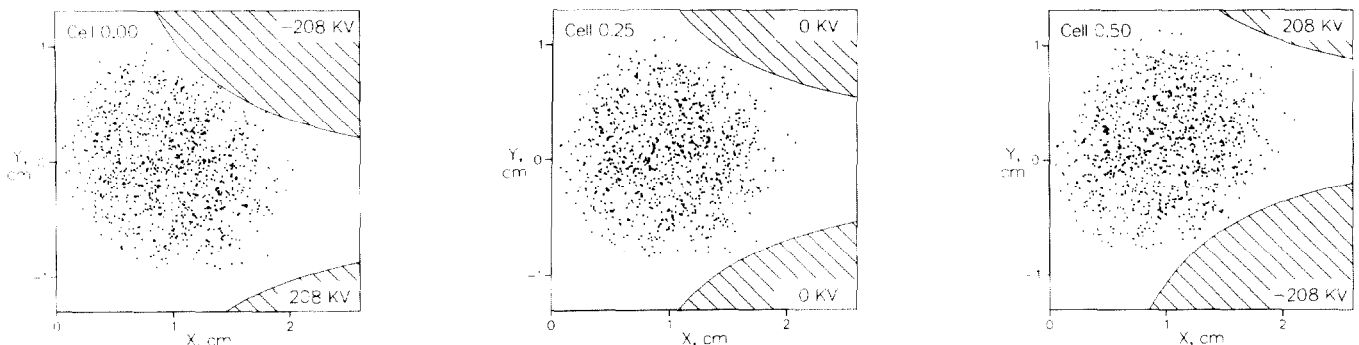


Fig. 2. Particles and pole tips at $z = 0, z = \beta\lambda/4$, and $z = \beta\lambda/2$.

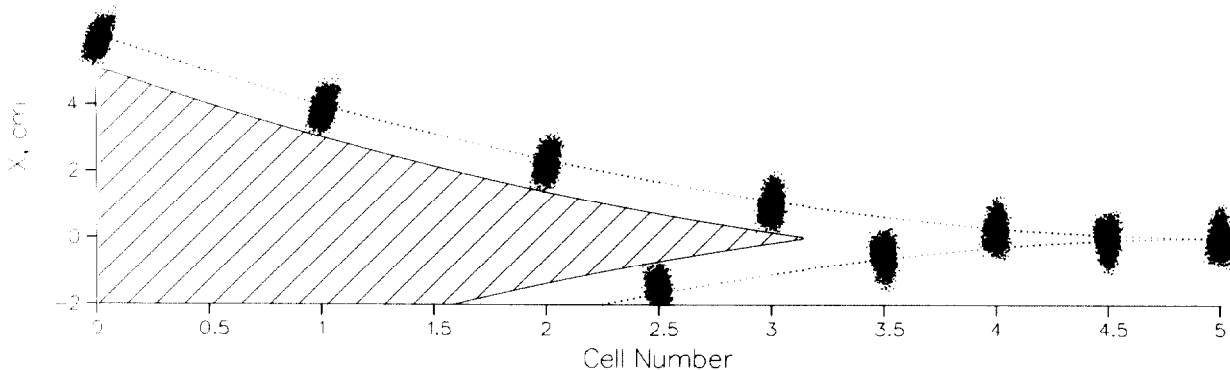


Fig. 3. Bunch trajectories. Grounded conductor is hatched; pole tips are not shown.

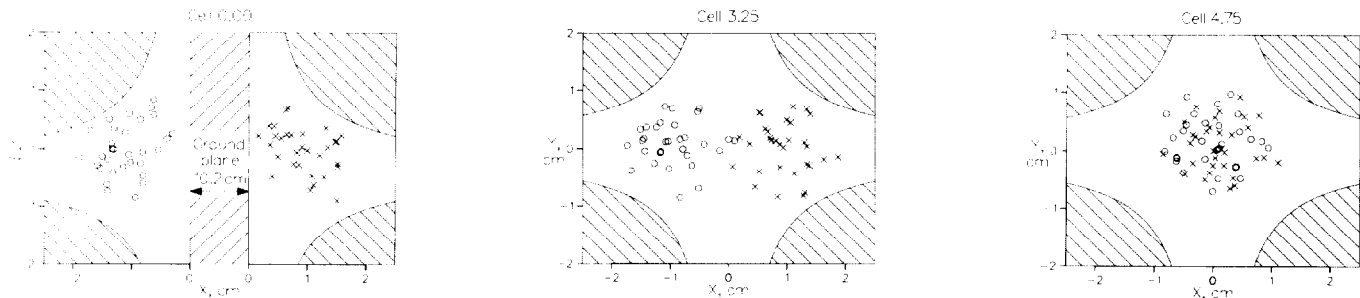


Fig. 4. Particles merging to final axis.

curvature and focusing strength. The peak surface electric field is approximately $1.36 \text{ V}/(\text{a}\sqrt{\text{m}}) = 17 \text{ MV/M}$ (Ref. 4).

The length of the funnel is $5\beta\lambda = 2.15$ meters. Beams enter the funnel at an angle of about 3° to the final axis and are deflected around the curve by the dipole component of E_x . For the first part of the funnel, beams follow the curvature of the poles and ground plane. At the end of the ground plane at $3.17\beta\lambda$, beams are about 1 cm away from the final axis at an angle of 1.24° . At this point, there is a discontinuity of 1.24° in the slope of the poles so that the poles are parallel to each other for the rest of the funnel. The beams are still subject to the dipole component of E_x . The curves of their trajectories are tangent to the final axis at $5\beta\lambda$ so that the beams merge at that point.

Certain field perturbations have been omitted and are believed to be negligible: fringe fields at the funnel ends, field errors from the curvature of the z -axis, bunch-bunch fields, and field errors at the ground plane vertex. As particles pass the end of the ground plane, the images of the pole tips in the ground plane coincide with the real pole tips on the other side except for the 1.24° angle shift. Because of the symmetry of the potential function, the electric fields should not be affected by the end of the ground plane except for the small angle shift perturbation, which should extend only a centimeter or so along the beamline from the end of the ground plane. Small deflection errors can be compensated by small changes in V , input steering, or changes in the dc potential of the RF ground plane.

Results

Bunch trajectories are shown in Fig. 3 in relation to the ground plane. The bunch is foreshortened in the z -direction (along the beam axis) because of the plot scale. Bunch-shape distortion resulting from nonlinear z -focusing is apparent in this plot. Funnel input ($z=0$) and output ($z=5\beta\lambda$) beam parameters are given in Table II. Emittances are rms, normalized. Emittance growth and particle losses are small.

Figure 2 shows the x - y projection of the bunch, the pole tips for the first half-cell of the funnel, and the distribution of the bunch within the aperture. As the synchronous particle moves down the beamline, it sees the pole tips at symmetric positions as the RF voltage passes through zero at

TABLE II. Beam Parameters.

	Input	Output
# particles	1000	974
$x_{\text{rms}}, \text{cm}$	0.364	0.397
$y_{\text{rms}}, \text{cm}$	0.438	0.467
$z_{\text{rms}}, \text{cm}$	1.249	1.191
$\epsilon_x, \text{cm-mrad}$	0.0180	0.0189
$\epsilon_y, \text{cm-mrad}$	0.0180	0.0185
$\epsilon_z, \text{cm-mrad}$	0.0234	0.0242

$\beta\lambda/4$ and $3\beta\lambda/4$ and sees the tips at their extreme positions at the beginning and halfway through the cell ($\beta\lambda/2$) at the RF voltage peaks. Figure 4 shows a few randomly selected particles from bunches on both sides of the ground plane at the funnel entrance, just after the ground plane ends and as they merge on the final axis.

Acknowledgments

We thank Tarlochan Bhatia for the preliminary RFQ design and the particle output from the PARMTEQ run. We are indebted to Michael Pabst for developing the Green's function for the potential generated by a point charge outside a conducting cylinder (Eq. 5).

References

1. J. E. Stovall, F. W. Guy, R. H. Stokes, and T. P. Wangler, "Beam Funneling Studies at Los Alamos," Proc. Heavy Ion Inertial Fusion Workshop, Darmstadt, June 1988, to be published, Los Alamos National Laboratory report LA-UR-88-3277 (1988).
2. R. H. Stokes and G. N. Minerbo, "Proposed Use of the Radio-Frequency Quadrupole Structure to Funnel High-Current Ion Beams," IEEE Trans. Nucl. Sci. **32**, 2593 (1985).
3. R. H. Stokes and G. N. Minerbo, "Scheme to Funnel Ion Beams with a Radio-Frequency Quadrupole," Proc. Workshop on High Current, High Brightness, and High Duty Factor Ion Injectors, La Jolla, CA, 1985, American Institute of Physics Conf. Proc. **139**, 79 (1986).
4. K. R. Crandall, R. H. Stokes, and T. P. Wangler, "RF Quadrupole Beam Dynamics Design Studies," Proc. 10th Linear Accelerator Conf., Brookhaven National Laboratory report BNL-51134, 205 (1979).